LA-UR-19-29126
Approved for public release; distribution is unlimited.

Title: Microstructural Characterization of High Dose Irradiated HT9

Author(s): Gigax, Jonathan Gregory
Kim, Hyosim

Intended for: Report

Issued: 2019-09-11

Microstructural Characterization of High Dose Irradiated HT9

Fuel Cycle Research & Development

Prepared for
U.S. Department of Energy
Advanced Fuels Campaign

Jonathan G. Gigax
Hyosim Kim

08/26/19

SUMMARY

The present report provides a short summary of the recent efforts to irradiate various HT9 heats and compositions to a high damage level (>500 peak dpa) and characterize the changes to the microstructure. The majority of the data reported here will focus on characterizing the "INL" HT9 heat. This particular heat was chosen due to its high volume fraction of tempered martensite (>90%) in the microstructure. The results show that very little swelling is present in INL HT9 up to doses up to 600 peak dpa. Voids are only observed in the near surface region. Some carbides are also observed to accompany the irradiation. Comparison of void swelling with published neutron irradiation shows good agreement. Additional investigations into the response of delta ferrite grains show a very different distribution of voids and significantly higher void swelling compared to the tempered martensite grains.

TABLE OF CONTENTS

FIGURES

TABLES

Intentionally Blank

1. Introduction

HT9 is a candidate ferritic/martensitic (F/M) fuel cladding material for next generation fast reactors. Originally developed for use as tubing material in high temperature applications, the very low void swelling observed from neutron irradiation and ion irradiation makes this material a promising candidate [1,2]. However, there is currently no data for void swelling of HT9 at 500-600 dpa, levels expected to be reached at end-of-life conditions for target burnups in fast reactors. Ion irradiation has been used as a surrogate for neutron irradiations due to its higher dpa rates. While this method does not give one-to-one swelling with neutron irradiated specimens, its higher dpa rate enables a significantly higher testing throughput and screening of materials. In this study, we utilize heavy ion irradiation to achieve damage levels up to 800 peak dpa to understand microstructural changes to HT9, namely void swelling, at damage levels not yet reached under reactor conditions.

2. Materials and Methods

One heat of HT9, termed the INL heat, with a composition given in Table 1 was annealed at 1040 °C for 30 min, air cooled, and followed by additional annealing at 760 °C for one hour and air cooled. Specimens were prepared for irradiation by electropolishing the surface with a solution of 5 vol.% perchloric acid and 95 vol.% methanol. The samples were irradiated with 3.5 MeV Fe ions at the Texas A&M University Radiation Materials Characterization Laboratory and Facility using a 1.7 MV IonX tandetron. The INL HT9 was irradiated at a temperature of 450 C to damage levels of 200, 600, and 800 peak dpa. Damage levels were calculated using the SRIM-2013 software package and a displacement energy of 40 eV [refs]. A static, defocused beam was used to avoid the influence of rastering on void swelling [3]. Cryotraps and a magnetic filtering magnet were used to remove contaminants from the beam line and chamber in an effort to avoid composition modification by carbon injection [3].

Table 1. Chemical composition of the INL HT9

Alloy ID	Fe	Cr	Mo	Si	Mn	Si	Ni	V	W	C
C26M	bal	12.5	1.1	0.29	0.41	0.2	0.6	0.3	0.51	0.21

A Tescan LYRA focused ion beam mill (FIB) was used to perform conventional cross-section lamella lift-out and thinning for transmission electron microscopy (TEM). After thinning the specimen to a thickness less than 100 nm, the micrographs of the lamella were obtained on a FEI Tecnai F20 ST operated at 200 kV in scanning transmission electron mode (STEM) with a high angle annular dark field detector (HAADF). Thickness of the lamella were measured using conventional electron energy loss spectroscopy.

3. Results and Discussion

3.1 Irradiation Effects on the Microstructure

Figure 1 provides a STEM micrograph of the INL HT9 after heat treatment. It is clear from the image that a majority of the grains are tempered martensite. A few delta ferrite grains were noted but are not visible in Fig. 1 due to their low volume fraction (~5-8%).

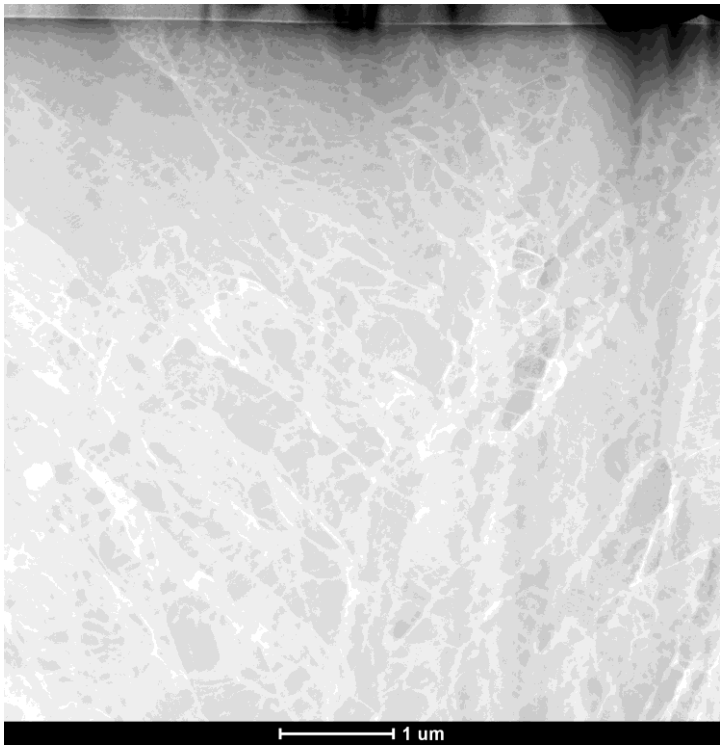

Figure 1 – STEM-HAADF micrograph of the unirradiated HT9 examined in the current study.

One of our main objectives in this study is to determine whether or not INL HT9 showed heavy ion-induced swelling up to doses of 800 peak dpa. We ignore, for now, any dislocation or precipitate analysis in the specimens after irradiation (although the latter will be briefly covered). Fig. 2 shows a brightfield and darkfield image of INL HT9 after irradiation to 600 peak dpa.

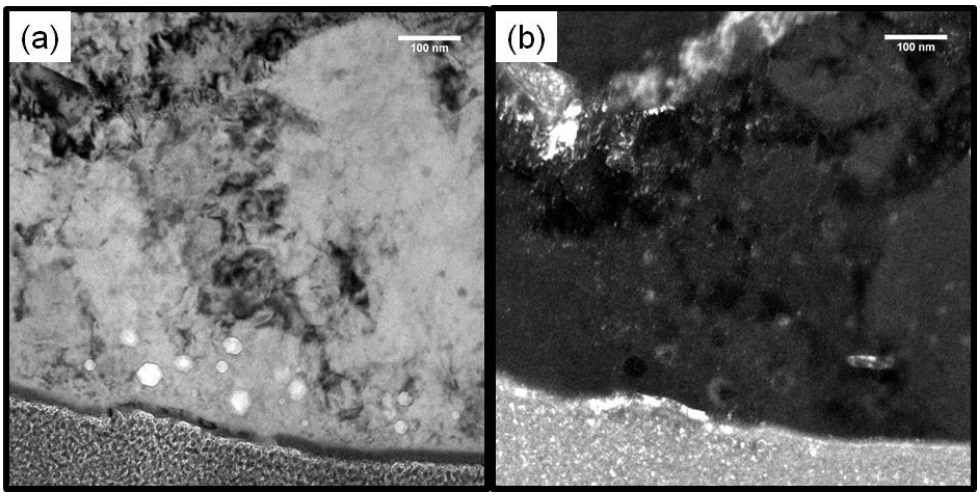

Figure 2 – (a) Brightfield and (b) darkfield TEM micrographs of INL HT9 irradiated to 600 peak dpa.

From Fig. 2 it is clear that void swelling is present in the material. However, the voids appear only near the surface and do not extend deeper into the sample. We further note that there are some precipitates present near the voids in the ion irradiated region and were identified as carbides. Analysis shown in the following section indicates that these are likely from a phenomenon of radiation-induced precipitation and not from carbon injection.

Fig. 3 provides a void swelling distribution plot for the damage levels investigated in this study. Void swelling values were measured from TEM micrographs and calculated using $V_{swelling} = \frac{V_{voids}}{V_{matrix} - V_{voids}} * 100$, where V_{voids} and V_{matrix} are the volumes of voids and matrix, respectively. Statistics were binned into 100 nm depth regions to provide depth-dependent swelling information.

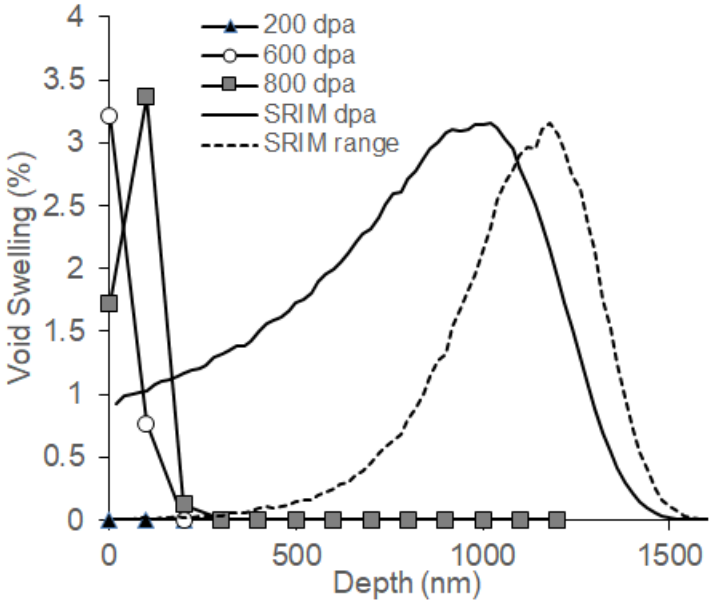

Figure 3 – Void swelling distributions for the INL HT9 irradiated to 200, 600, and 800 peak dpa.

By itself, Fig. 3 does not necessarily provide much meaningful data beyond two key observations. First, swelling increases significantly from 200 to 600 peak dpa but does not increase at a commensurable rate from 600 to 800 peak dpa. Second, the depth of the voids shifts deeper with increasing dose, but does not extend below a depth of 300 nm. To provide some legitimacy to this result, we compare the void swelling statistics obtained in this study to that measured in specimens irradiated in the Fast Flux Test Facility (FFTF) [1,2]. From Fig. 4, the void swelling data obtained in this study has good agreement with the results from neutron irradiation in FFTF. We note that this is far short of the 0.2%/dpa swelling observed in body centered cubic iron alloys [8]. This result implies that swelling has not quite reached a steady state and irradiations to higher doses are needed to determine if HT9 will reach a 0.2%/dpa steady state swelling rate.

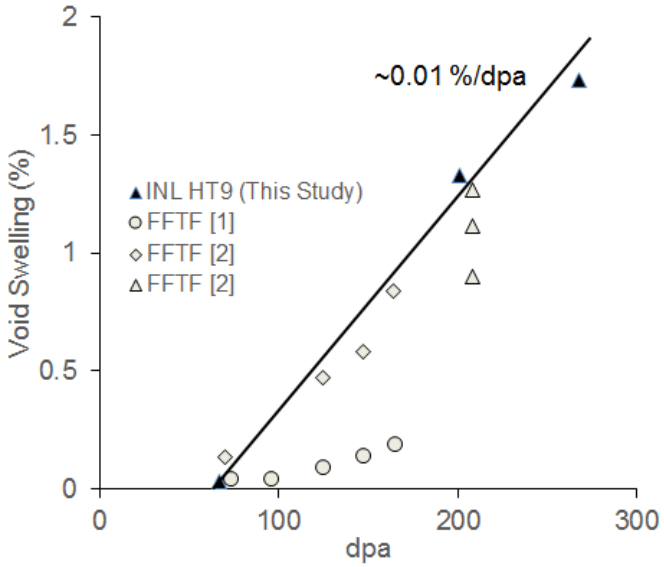

Figure 4 – Comparison of heavy-ion induced void swelling in INL HT9 (this study) and void swelling from irradiation in FFTF [1,2].

3.2 Irradiation-Induced Precipitation

A closer examination of Fig. 2 shows the formation of precipitates after ion irradiation. A small effort was taken to quantify this and is provided in Fig. 5 below. Based on high resolution TEM and diffraction analysis, it was concluded that the precipitates are some form of carbide (i.e. M23C6, M7C3, etc.) and more detailed analysis is given in [6]. We note that quantification from by TEM is not necessarily reflective of the total amount of carbon as this method is unable to determine the amount of carbon remaining in solution. From our previous study, secondary ion mass spectroscopy was performed and showed that the INL HT9 irradiated to 600 peak dpa had nearly the same amount of carbon in the matrix as the unirradiated HT9 specimen [3].

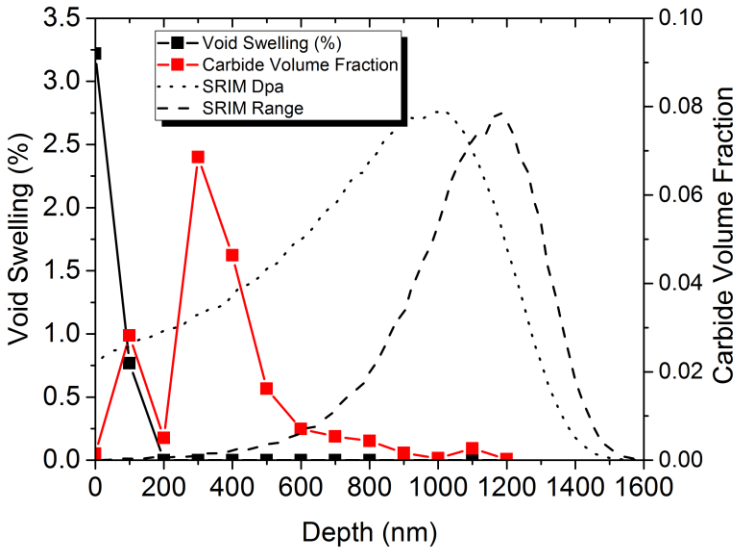

Figure 5 – Void swelling and carbide volume fraction distribution in the INL HT9 irradiated to 600 peak dpa.

Fig. 5 shows carbide formation similar to the carbon profile measured in from SIMS. This particular trend is interesting as it follows void swelling distributions measured in pure Fe and is located near where vacancies have the highest density [9]. We also note that the large amount of swelling observed near the surface is characteristic of the defect imbalance effect where vacancies also have a higher concentration than interstitials near the surface. It is well known that carbon is a fast diffusing element in iron systems, with a few carbon atoms capable of occupying a vacancy site in the matrix. It is not surprising, then, to see carbide formation in this area. However, we note that the rate of carbon precipitation may or may not be similar to that observed in neutron irradiated specimens. This aspect of irradiation merits further investigation to determine if it is a neutron atypical phenomenon in ion irradiated materials.

3.3 Ferrite vs. Martensite Void Swelling

Although the tempered martensite grains comprise the vast majority of the matrix, we extended our investigation to the delta ferrite grains in the matrix. These grains have a different chemical composition (i.e. higher carbon) and structure (i.e. no lathe boundaries), so the comparison of void swelling needs to consider both of these aspects. Fig. 6 provides micrographs of the void swelling in the delta ferrite grains at 200 and 600 peak dpa, respectively. At 200 peak dpa, there are a few small voids that appear near the surface and to a depth of ~500 nm. At 600 peak dpa, it is very clear that the swelling in the delta ferrite grain is significantly larger due to both a higher density of voids and larger voids. Furthermore, voids are observed deeper below the ion-incident surface to a depth of ~700 nm, with a few voids appearing deeper.

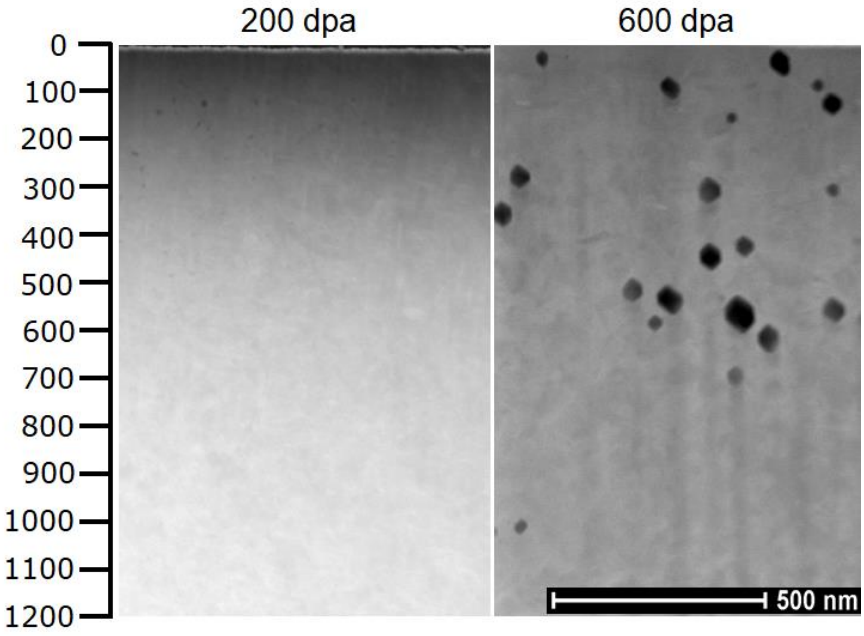

Figure 6 – Void swelling in delta ferrite grains after irradiation to 200 and 600 peak dpa.

Fig. 7 provides a comparison of the void swelling distribution measured in the tempered martensite and delta ferrite grains at 600 peak dpa. Similar to observations made above, the void swelling in the ferrite clearly extends deeper than the tempered martensite and is significantly higher overall. We note

that carbide formation was observed in the delta ferrite grains with a higher density than that observed in the tempered martensite.

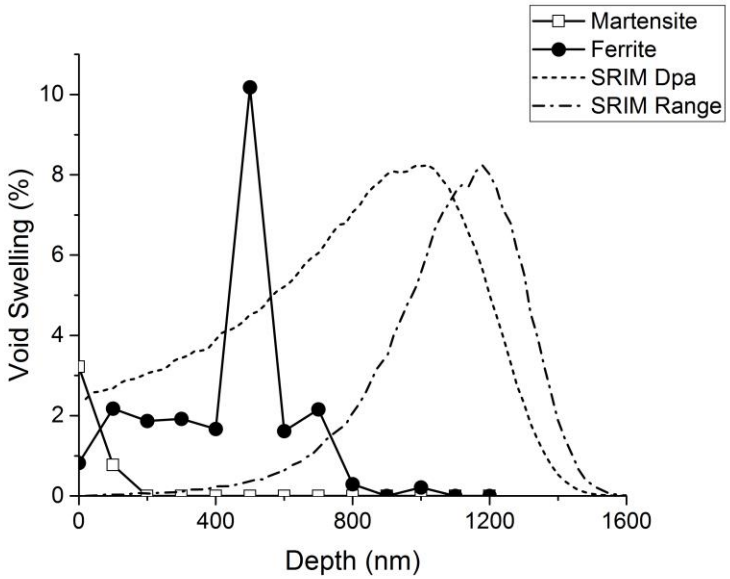

Figure 7 – Void swelling distribution in tempered martensite and delta ferrite grains after irradiation 600 peak dpa.

From these results, we speculate that one of the main sources of the difference in swelling of the tempered martensite and delta ferrite grains is the dislocation content. From our initial survey, the carbide density is higher in the delta ferrite than the tempered martensite. If radiation-induced precipitation was one of the major mechanisms for the suppression of void swelling, we would expect the delta ferrite to swelling less. Coupled with the higher starting carbon content of the grain and it is unlikely that carbon, by itself, is the largest contributor to the difference. Instead, if we consider the fact that tempered martensite has a much high dislocation content and density of low angle grain boundaries (i.e. lathes), then this aspect is likely the source of the difference. Although high dislocation/low angle grain boundary content has been shown to cause higher swelling in the material, usually due to the unstable nature of the microstructure, it is uncertain if this applies to tempered martensite grains in HT9 [8]. Grains did not appear to change size after irradiation, suggesting that microstructure is quite stable under irradiation. For future experiments, we have identified an alloy of HT9 that is purely ferritic in nature. High dose irradiations are planned for these two alloys such that the only difference between the INL HT9 heat and the ferritic HT9 alloy void swelling will be caused by the dislocation content.

4. Conclusions and Future Work

In this study, we performed heavy ion irradiation on a variety of HT9 heats to high damage levels. We closely examined the INL HT9 heat and found that the tempered martensite grains showed little swelling, even at the highest dose, with a majority of the voids located near the ion-incident surface. A maximum void swelling of 3.2% was measured in the near surface region. Comparisons with neutron irradiation data showed good agreement with swelling trend measured in the ion irradiated specimens.

Some amount of radiation-induced precipitations was observed in the irradiated specimens. The volume fraction distribution of the carbides closely matched the SIMS measured carbon concentration profile, suggesting that these formed from excess vacancies in that depth region. It is not clear at this time whether or not precipitate formation effectively suppressed void swelling at deeper depths in the tempered martensite grains.

A large amount of swelling was observed in delta ferrite grains. Furthermore, voids appeared to depths up to the dpa peak and near the end of ion range. Carbides and precipitates were also observed to appear in the grains as well. There are two notable differences between delta ferrite and tempered martensite: chemical composition and dislocation/grain boundary density. From the initial data we have obtained, it appears that the dislocation content is the main contributor to the difference in swelling. To test this speculation, our plan involves irradiating a fully ferritic HT9 alloy with a similar chemical composition as the INL HT9 heat in this study. The only difference between these alloys will be the dislocation content.

Our irradiation matrix included more than just the INL HT9 heat. We also examined three other HT9 alloys, AC03, and a low and high nitrogen content HT9, irradiated to 600 peak dpa. We note that these alloys all showed a variety of responses but one common feature in all was the formation of dense carbides in the irradiated region. A delta ferrite grain was examined in the AC03 heat and no swelling was observed. Work is still ongoing to determine where the source of carbon was for these materials and if adjustments to specimen preparation need to be made.

5. References

1. M.B. Toloczko, F. A Garner, C. R. Eiholzer, Irradiation creep and swelling of US fusion heats of HT9 and 9Cr-1Mo to 208 dpa at ~400 C, J. Nucl. Mater. 212-215 (1994) 604-607.
2. M.B. Toloczko and F. A Garner, Irradiation creep and void swelling of two LMR heats of HT9 at~400°C and 165dpa, J. Nucl. Mater. 233-237 (1996) 289-292.
3. J. G. Gigax, E. Aydogan, T. Chen, D. Chen, L. Shao, Y. Wu, W. Y. Lo, Y. Yang, and F. A. Garner, The influence of ion beam rastering on the swelling of self-ion irradiated pure iron at 450°C, J. Nucl. Mater. 465 (2015) 343–348.
4. J.F. Ziegler, M.D. Ziegler, J.P. Biersack, SRIM: The stopping and range of ions in matter, Nucl. Instr. Methods Phys. Res. B 268 (2010).
5. R. Stoller, M.B. Toloczko, G.S. Was, A.G. Certain, S. Dwaraknath, F.A. Garner, On the use of SRIM for computing radiation damage exposure, Nucl. Methods Phys. Res. Sect. B 310 (2013) 75-80.
6. J. G. Gigax, H. Kim, E. Aydogan, F. A. Garner, S. A Maloy, and L. Shao, Beam-contamination-induced compositional alteration and its neutron-atypical consequences in ion simulation of neutron-induced void swelling, Mater. Res. Lett. 5 (2017) 478-485.
7. J. G. Gigax, T. Chen, H. Kim, J. Wang, L. M. Price, E. Aydogan, S. A. Maloy, D. K. Schreiber, M. B. Toloczko, F. A. Garner, and Lin Shao, Radiation response of alloy T91 at damage levels up to 1000 peak dpa, J. Nucl. Mater. 482 (2016) 257-265.
8. J. G. Gigax, H. Kim, T. Chen, F. A. Garner, and L. Shao, Radiation instability of equal channel angular extruded T91 at ultra-high damage levels, Acta Mater. 132 (2017) 395-404.
9. L. Shao, C-C. Wei, J. G. Gigax, A.Aitkaliyeva, D. Chen, B. H. Sencer, and F. A. Garner, Effect of defect imbalance on void swelling distributions produced in pure iron by 3.5 MeV self-ions, J. Nucl. Mater. 453 (2014) 176–181.